

Learning Neural Controllers with Optimality and Stability Guarantees Using Input-Output Dissipativity

Han Wang^{a,b}, Keyan Miao^b, Diego Madeira^b, Antonis Papachristodoulou^b

^a*Automatic Control Laboratory (IfA), ETH Zürich, Zürich, Switzerland*

^b*Department of Engineering Science, University of Oxford, OX1 3PJ, Oxford, UK*

Abstract

Deep learning methods have demonstrated significant potential for addressing complex nonlinear control problems. For real-world safety-critical tasks, however, it is crucial to provide formal stability guarantees for the designed controllers. In this paper, we propose a new framework for designing neural controllers that achieve both stability and optimality with respect to certain functions. Our key idea is to exploit the concept of input-output dissipativity of nonlinear systems by learning neural storage functions and supply rate functions. As a generalization of Lyapunov theory, dissipativity theory provides a natural connection to optimal control theory, offering both stability guarantees and meaningful optimality certificates. The neural controllers can be directly derived from the learned supply rate functions and guarantee closed-loop stability while inheriting optimality properties that can be shaped towards user-defined control objectives. Extensive numerical experiments demonstrate the effectiveness of our approach.

Key words: Learning based control, optimal control, deep learning, dissipativity

1 Introduction

In recent years, deep learning has become a prevalent method for complex nonlinear control tasks, including robotics [1], intelligent transportation [2], power systems [3], and others. While these learning-based methods effectively handle complex control tasks that challenge traditional approaches, they in general come with no formal guarantees of desired properties, such as stability.

In control theory, Lyapunov's second method [4] is a widely used method for analyzing stability by designing an energy-like Lyapunov function. Stability is certified if this function strictly decreases along closed-loop tra-

jectories. However, constructing such a function is non-trivial. For polynomial or polynomial-transformable systems, sum-of-squares programming can be used to design stabilizing control laws and Lyapunov functions [5–8]. Yet, this approach is only immediately applicable to polynomial systems and it is known that some stable polynomial systems may lack a global polynomial Lyapunov function [9].

Learning-based methods for neural controllers and Lyapunov functions is a promising alternative approach [10–15]. To ensure formal guarantees, these methods employ a counterexample-guided inductive synthesis framework [16], with stability verified via tools such as Satisfiable Modulo Theories (SMT) [17], bound propagation [18], mixed-integer programming [19], and semi-definite programming [20]. While effective for stabilizing control, these approaches may not optimize performance metrics like cumulative energy consumption, as neural controllers are trained over *samples* rather than *trajectories*. This somewhat myopic design lacks infinite-horizon optimality. To bridge this gap, in this paper we develop neural controllers that not only ensure stability but also provide guaranteed optimality over an infinite horizon.

The key technology we are using is dissipativity theory [21], which generalizes Lyapunov theory with gen-

* Keyan Miao and Han Wang contributed equally. Keyan Miao acknowledges support from the Engineering and Physical Sciences Research Council (EPSRC) under project EP/T517811/1, Diego Madeira acknowledges XXXX, Antonis Papachristodoulou acknowledges support from the Engineering and Physical Sciences Research Council grants EP/Y014073/1 and EP/X031470/1.

Email addresses: hanwang@control.ee.ethz.ch (Han Wang), keyan.miao@eng.ox.ac.uk (Keyan Miao), diego.madeira@eng.ox.ac.uk (Diego Madeira), antonis@eng.ox.ac.uk (Antonis Papachristodoulou).

eralized energy functions, namely storage functions and supply rate functions that depict energy dissipation for input-output pairs. Similarly to Lyapunov’s method, dissipativity theory can also be used to certify stability and design stabilizing controllers. A key advantage of dissipativity-based control is its inherent optimality over an infinite horizon [22,23]. Recent work has applied this to stochastic nonlinear systems, assuming fixed storage and supply rate functions for Lyapunov-type stabilizing control [24]. For more flexible and practical design, one can consider learning these functions, though this is even more challenging than Lyapunov function design. The difficulty arises because *dissipativity is an input-output property*, whereas *Lyapunov stability is a state property*. From a learning perspective, this requires sampling over the product of input and output spaces, making the problem especially difficult for multi-input multi-output systems. To address this, we propose a novel reformulation of the dissipativity condition that depends only on the output space, reducing the sampling space’s dimensionality.

Previous work on analyzing and learning dissipativity, as well as designing feedback controllers, includes the following. For polynomial systems, sum-of-squares programming has been used to design polynomial storage functions and quadratic supply rate functions [25, 26], making it more applicable to polynomial dynamics, similar to Lyapunov functions. Recently, neural proportional-integral control based on equilibrium-independent passivity was proposed [27], but it assumes known storage and supply rate functions and strictly passive open-loop systems. A similar approach was adopted in [28] for dissipativity certification, though it relies on simple quadratic parameterizations. Learning dissipative neural dynamics has been explored in [1, 29–31], but these works do not address the more challenging problem of control design.

Our main contributions are:

- We propose a new framework for designing neural control with provable stability guarantees by learning input-output dissipativity. The resulting control law stabilizes *any* system sharing the same dissipativity property;
- We prove that the designed neural control is the optimal solution to an infinite-horizon optimal control problem, with the cost functional learned based on user-defined objectives;
- We reformulate the dissipativity conditions to reduce the dimensionality of the sampling space, enabling more efficient learning of neural storage and supply rate functions;
- We validate the stability and optimality of our method through numerical experiments, demonstrating superior performance over neural Lyapunov-based control in optimality.

The paper is organized as follows. Section 2 formulates the problem of designing optimal and stabilizing control laws and outlines key challenges. Section 3 presents our approach to neural control design via input-output dissipativity. The training and formal verification algorithm is detailed in Section 4, followed by experimental validation in Section 5.

2 Problem Statement

Consider a plant with the following nonlinear dynamics

$$\dot{x}(t) = f(x(t)) + g(x(t))u(t) \quad (1)$$

where $x(t) \in \mathcal{X} \subset \mathbb{R}^n$ is the state and $u(t) \in \mathcal{U} \subset \mathbb{R}^m$ is the control input. We assume that the state $x(t)$ of system (1) can be measured for any time $t \geq 0$. Functions $f(x) : \mathcal{X} \rightarrow \mathbb{R}^n$ and $g(x) : \mathcal{X} \rightarrow \mathbb{R}^{n \times m}$ are assumed to be locally Lipschitz continuous on the compact set \mathcal{X} which has a non-empty interior.

2.1 Stabilizing Control

The primary goal of this paper is to design a locally Lipschitz continuous state-feedback controller $\pi(x(t))$ that *stabilizes* the plant (1) around the equilibrium point $x^* \in \mathbb{R}^n$. Note that local Lipschitz continuity is essential for local solution uniqueness and existence of the ODE $\dot{x} = f(x) + g(x)\pi(x(t))$. The key to prove local asymptotic stability of the equilibrium points of nonlinear systems is the existence of local Lyapunov functions.

Definition 1 (Local Lyapunov Function) *Consider the system (1) with a locally Lipschitz continuous controller $u(t) = \pi(x(t))$, and a compact set $\mathcal{X} \subset \mathbb{R}^n$ that contains x^* . A function $V(x) : \mathcal{X} \rightarrow \mathbb{R}$ is called a Lyapunov function for the system if it satisfies*

$$\begin{aligned} V(x^*) &= 0, \quad V(x) > 0, \forall x \in \mathcal{X} \setminus \{x^*\} \\ \dot{V}(x) &= \frac{\partial V(x)}{\partial x} [f(x) + g(x)\pi(x)] < 0, \forall x \in \mathcal{X} \setminus \{x^*\}. \end{aligned} \quad (2)$$

As a consequence of $f(x^*) + g(x^*)\pi(x^*) = 0$, we have $\dot{V}(x)|_{x=x^*} = 0$. From the Lyapunov’s direct method, the existence of a local Lyapunov function ensures local asymptotic stability of the system (1) with control $u(t) = \pi(x(t))$. This motivates the definition of *stabilizing control*.

Definition 2 (Stabilizing Control) *Consider the system (1). The locally Lipschitz continuous control $\pi(x(t))$ is called a stabilizing control, if it stabilizes the nonlinear system asymptotically.*

2.2 Optimal Control

Another problem of interest is optimality. The asymptotically stable optimal control problem is given as follows:

$$\begin{aligned} u^*(t) = \arg \min_{u(\cdot)} \int_0^\infty l(x, u) dt \\ \text{subject to } \dot{x} = f(x) + g(x)u \\ \lim_{t \rightarrow \infty} x(t) = 0 \end{aligned} \quad (3)$$

Here, the cost function $l(x, u) : \mathbb{R}^{n \times m} \rightarrow \mathbb{R}_+$ is the metric for control performance. Take linear quadratic regulator (LQR) problems as an example: the cost function $l(x, u) = x^\top Qx + u^\top Ru$ consists of terms related to state deviations and control effort. The two constraints are clear, one for system evolution and one for stability [32]. We are now at the stage of defining *optimal stabilizing control*.

Definition 3 (Optimal Stabilizing Control) Consider System (1). The locally Lipschitz continuous control $\pi(x(t))$ is called an optimal stabilizing control law if it is the optimal solution of some optimal control problem (3), i.e. $u^*(t) \equiv \pi(x(t))$.

In control theory, optimal control is widely used for its long-term optimal performance formulation. However, solving (3) is arduous for nonlinear systems, even with a quadratic cost functional. Problem (3) is an infinite optimization problem, of which the exact solution requires solving the computationally expensive Hamilton-Jacobian-Bellman equation.

2.3 Design Goal

We aim to design a neural control $\pi(x(t))$ as the optimal solution to an infinite-horizon optimal control problem (3) for general nonlinear systems, ensuring both optimality and stability by design.

3 Methodology

As discussed in Section 1, previous works learn a neural controller with stability guarantees but do not consider optimality [10–15]. In this section, we present the theoretic control design framework, then prove stability and optimality of the designed control. Without loss of generality, we consider $x^* = 0$, i.e., stabilization around the origin, in the sequel. The results can be easily extended to the case where $x^* \neq 0$.

3.1 Control with Stability Guarantees

The key technology we are using is *dissipativity theory*, as a generalization to Lyapunov theory.

Definition 4 (Dissipativity) Consider system (1). The system is called dissipative if there exist functions $V(x) : \mathcal{X} \rightarrow \mathbb{R}$ and $w(x, u) : \mathcal{X} \times \mathcal{U} \rightarrow \mathbb{R}$, such that

$$V(0) = 0, \quad V(x) > 0, \forall x \in \mathcal{X} \setminus \{0\}, \quad (4a)$$

$$\frac{\partial V(x)}{\partial x} [f(x) + g(x)u] \leq w(x, u), \forall x \in \mathcal{X}, u \in \mathcal{U}. \quad (4b)$$

$V(x)$ is called a *storage function*, which formulates the totally (nonnegative) energy storage of the system (1), as a generalization of Lyapunov functions. $w(x, u)$ is called *supply rate function*, which represents the supply rate that can be ‘tolerated’ or ‘dissipated’ by the system.

Dissipativity provides a nice insight for designing stabilizing controllers. Intuitively, if a system is dissipative with a storage function $V(x)$ and a supply rate function $w(x, u)$, the controller $\pi(x)$ should be designed such that

$$w(x, \pi(x)) < 0, \forall x \in \mathcal{X} \setminus \{0\}. \quad (5)$$

Then, the closed-loop system $\dot{x} = f(x) + g(x)\pi(x)$ is naturally stable as $V(x)$ is a Lyapunov function. The following theorem is the main result of this paper. It proposes a *structure* of the controller $\pi(x)$ that always satisfies (5).

Theorem 5 Consider system (1), a storage function $V(x)$ and a supply rate function

$$w(x, u) = x^\top Q(x)x + 2x^\top S(x)u + u^\top R(x)u \quad (6)$$

where $Q(x) : \mathcal{X} \rightarrow \mathbb{R}^{n \times n}$, $S(x) : \mathcal{X} \rightarrow \mathbb{R}^{n \times m}$, $0 \prec R(x) : \mathcal{X} \rightarrow \mathbb{R}^{m \times m}$, $\forall x \in \mathcal{X}$ that satisfy (4). If

$$\Delta(x) := S(x)R(x)^{-1}S(x)^\top - Q(x) \succ 0, \forall x \in \mathcal{X}, \quad (7)$$

then with

$$\pi(x) = -R(x)^{-1}S(x)^\top x, \quad (8)$$

the condition (5) always holds. $\pi(x)$ is a stabilizing control for the system (1).

PROOF. The result provided in the theorem is based on the fact that if (4) holds with $R(x) \succ 0$ and $\Delta(x) \succ 0$, then by considering $u = \pi(x)$, where $\pi(x)$ is given in (8), it follows that

$$\dot{V}(x) \leq -x^\top \Delta(x)x < 0, \quad (9)$$

which is a closed-loop Lyapunov condition. Thus, the feedback control $\pi(x)$ asymptotically stabilizes the system around the origin. If $V(x)$ is radially unbounded and (4) is valid $\forall (x, u) \in (\mathbb{R}^n \times \mathbb{R}^m)$, then global asymptotic stability is achieved.

Necessity of the conditions mentioned in that theorem can be proved as well, although this is more involved. By assuming that a Lyapunov condition is verified for some $V(x) > 0$ and some control law given by

$$u(x) = Y(x)x \quad (10)$$

a solution to dissipation inequality (4) with $\Delta(x) = 0$ is guaranteed to exist. This means that there is a great degree of generality in the results of Theorem 5, which justifies its application in this work.

Firstly, let us suppose that for some control given by (10) we have

$$\nabla V(x)^\top [f(x) + g(x)u(x)] < 0. \quad (11)$$

In addition, assume that there exists some $\bar{M}(x)$ such that

$$\nabla V(x) = \bar{M}(x)x, \quad (12)$$

which can be considered without loss of generality. Then, it also follows that

$$\nabla V(x)^\top [f(x) + g(x)\hat{u}(x)] + \quad (13)$$

$$\nabla V(x)^\top g(x) \frac{\beta(x)}{4} g(x)^\top \nabla V(x) < 0, \quad (14)$$

with

$$\hat{u}(x) = K(x)x, \quad K(x) = \left(Y(x) - \frac{\beta(x)}{4} \bar{M}(x) \right). \quad (15)$$

Stability condition (13) leads to

$$\begin{aligned} \nabla V(x)^\top f(x) < \\ - \nabla V(x)^\top g(x)K(x)x - \nabla V(x)^\top g(x) \frac{\beta(x)}{4} g(x)^\top \nabla V(x). \end{aligned} \quad (16)$$

At the same time, the *dissipativity* matrix condition (22) can be equivalently presented as

$$\begin{aligned} \nabla V(x)^\top f(x) < \\ x^\top Q(x)x - \nabla V(x)^\top g(x) \frac{R(x)^{-1}}{4} g(x)^\top \nabla V(x) \\ + \nabla V(x)^\top g(x)R(x)^{-1}S(x)^\top x - x^\top S(x)R(x)^{-1}S(x)^\top x. \end{aligned} \quad (17)$$

One can quickly verify that stabilizability implies dissipativity if the right-hand side of condition (16) is not greater than the right-hand side of (17). This is the case

if $R(x) = \beta(x)^{-1}I$,

$$S(x) = - \left[Y(x) - \frac{\beta(x)}{4} M(x) \right]^\top R(x),$$

$K(x) = -R(x)^{-1}S(x)^\top$ and $Q(x) = S(x)R(x)^{-1}S(x)^\top$, which means that $\Delta(x) = 0$.

The proof of Theorem 5 is based on Theorem 1 of [25]. It provides a powerful insight on the relationship between dissipativity theory and the problem of feedback stabilization. The main idea behind this approach is that a *storage function* may play the role of a *control-Lyapunov function* for the closed-loop system, if certain conditions on the supply rate are satisfied. This provides a great degree of flexibility in designing a controller when compared to passivity-based approaches, for example, where a passive structure must be imposed on the closed loop. In dissipativity-based control, instead, we analyze the open loop properties of the plant; no specific closed-loop behaviour, such as a Hamiltonian structure, needs to be guaranteed in order to obtain stability. \square

In Theorem 5, the supply rate function $w(x, u)$ is considered in the specific form (6), generalizing the so-called *QSR supply rate*, where $Q(x)$, $S(x)$, and $R(x)$ are constant matrices. While widely used in convex optimization-based control design [25], this formulation can make the dissipativity condition (4) conservative or intractable for general nonlinear systems. In Section 4, we show how to learn $V(x)$, $Q(x)$, $S(x)$, and $R(x)$ to provably satisfy (4).

So far we have proved that the structured control $\pi(x)$ in (8) can stabilize the system. In the next sub-section, we show that it also endows the closed loop system with a notion of optimality, as it is the optimal solution to an optimal control problem with a meaningful cost function.

3.2 Infinite-time Horizon Optimality Guarantees

The following theorem demonstrates optimality of $\pi(x)$ as in the form (8).

Theorem 6 *Consider the system (1), a storage function $V(x)$ and a supply rate function $w(x, u) = x^\top Q(x)x + 2x^\top S(x)u + u^\top R(x)u$, such that (4) and (7) hold. Then, $\pi(x) = -R(x)^{-1}S(x)^\top x$ is the optimal solution of the following optimal control problem with positive definite running cost:*

$$\begin{aligned} \min_{u(\cdot)} \int_0^\infty \left[\tilde{l}(x, u) + u^\top R(x)u + x^\top \Delta(x)x \right] dt \\ \text{s.t. } \dot{x} = f(x) + g(x)u \\ \lim_{t \rightarrow \infty} x(t) = 0 \end{aligned} \quad (18)$$

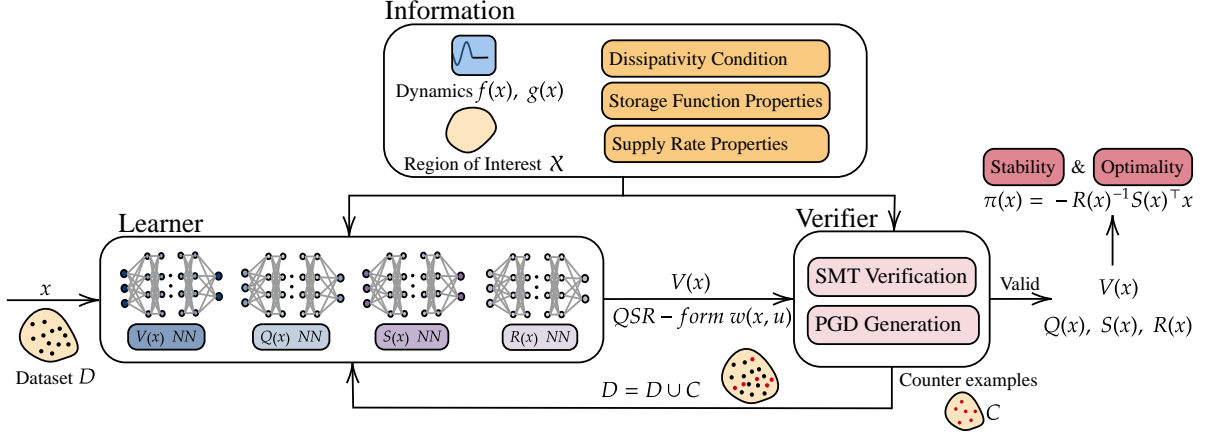


Fig. 1. Schematic of the verification-guided dissipativity learning framework for stabilizing and optimal control synthesis

where $\tilde{l}(x, u) = -\frac{\partial V(x)}{\partial x} f(x) - \frac{\partial V(x)}{\partial x} g(x)u + x^\top Q(x)x + 2x^\top S(x)u$. Moreover, the value function of (18) is $V(x)$.

PROOF. Substituting

$$v = u + R(x)^{-1} S(x)^\top x \quad (19)$$

into (18) and applying dynamic programming, we have

$$\begin{aligned} J &= \min_{u(\cdot)} \int_0^\infty [\tilde{l}(x, u) + x^\top R(x)x + x^\top \Delta(x)x] dt \\ &= -\min_{u(\cdot)} \int_0^\infty \dot{V}(x) dt + \min_{v(\cdot)} \int_0^\infty [w(x, u) + x^\top \Delta(x)x] dt \\ &= V(x(0)) - \lim_{T \rightarrow \infty} V(x(T)) + \min_{v(\cdot)} \int_0^\infty v^\top R(x)v dt \end{aligned}$$

Given that we are minimizing over these u such that $\lim_{t \rightarrow \infty} x(t) = 0$, we have $\lim_{T \rightarrow \infty} V(x(T)) = 0$. Moreover, since $R(x) \succ 0$ for any x , the minimum of $\min_{v(\cdot)} \int_0^\infty v^\top R(x)v dt$ is attained at $v = 0$. From (19), we obtain that the nonlinear control $u = -R(x)^{-1} S(x)^\top x$ is the optimal solution and the storage function $V(x)$ is the optimal value function.

We then show that the cost function of (18) is always positive definite. The cost function can be split into two terms: 1) $\tilde{l}(x, u) + u^\top R(x)u$ and 2) $x^\top \Delta(x)x$. Term 1) is positive semi-definite provided that (4b) holds, while term 2) is positive definite because $\Delta(x) \succ 0$ from (7). \square

The following proposition demonstrates that the cost functional of the optimal control problem becomes non-linear quadratic if an additional regularity condition is satisfied.

Proposition 7 Consider the system (1), a storage function $V(x)$ and a supply rate function $w(x, u) = x^\top Q(x)x + 2x^\top S(x)u + u^\top R(x)u$, such that (4), (7) and additionally

$$x^\top Q(x)x = \frac{\partial V(x)}{\partial x} f(x), \quad 2x^\top S(x)u = \frac{\partial V(x)}{\partial x} g(x). \quad (20)$$

hold. Then, $\pi(x) = -R(x)^{-1} S(x)^\top x$ is the optimal solution of the following optimal control problem:

$$\begin{aligned} \min_{u(\cdot)} \int_0^\infty [u^\top R(x)u + x^\top \Delta(x)x] dt \\ \text{s.t. } \dot{x} = f(x) + g(x)u \\ \lim_{t \rightarrow \infty} x(t) = 0 \end{aligned} \quad (21)$$

Moreover, the value function of (21) is $V(x)$.

The proof of Proposition 7 follows directly from Theorem 6, noting that $\tilde{l}(x, u) = 0$ when (20) holds.

The term $u^\top R(x)u$ represents the total energy consumption required to stabilize the system from $x(0)$, while $x^\top \Delta(x)x$ penalizes deviations from the origin. The cost function can be adjusted by tuning $R(x) \succ 0$, $\Delta(x)$, and $V(x)$. A larger $R(x)$ prioritizes control effort minimization, leading to smoother but slower convergence. Conversely, a smaller $R(x)$ emphasizes state deviation minimization, resulting in faster convergence but higher energy consumption.

4 Counterexamples Inductive Learning Algorithm

In this section, we present the main algorithm of designing the storage function $V(x)$ and the supply rate function $w(x, u) = x^\top Q(x)x + 2x^\top S(x)u + u^\top R(x)u$ that provably satisfy the conditions:

- Storage function properties:
 - $V(0) = 0$
 - The bi-Lipschitz condition: $\mu x^\top x \leq V(x) \leq \nu x^\top x, \forall x \in \mathcal{X}$
- QSR-form supply rate properties:
 - $R(x) \succ 0$
 - $\Delta(x) := S(x)R(x)^{-1}S(x)^\top - Q(x) \succ 0$
- The dissipativity condition:

$$\frac{\partial V(x)}{\partial x}[f(x) + g(x)u] \leq w(x, u), \forall x \in \mathcal{X}, u \in \mathcal{U}.$$

and additionally

- Cost functional shaping w.r.t. a user defined objective $l(x, u)$:

$$\tilde{l}(x, u) + u^\top R(x)u + x^\top \Delta(x)x \approx l(x, u), \forall x \in \mathcal{X}, \forall u \in \mathcal{U}$$

Figure 1 shows the learning structure. The main idea is to use the counter example guided inductive synthesis framework [16]. Our framework consists of two main components working together iteratively:

- A learning module that trains neural networks to represent $V(x)$, $Q(x)$, $S(x)$, and $R(x)$, optimizing over data samples to satisfy the required conditions. The learning is guided by carefully designed loss functions.
- A verification module that employs Satisfiability Modulo Theory (SMT) solvers to formally verify whether the learned functions satisfy all requirements. When violations are found, it generates counterexamples for improving the learned functions.

When the verifier finds a violation of any condition, the counterexample point is used by the learner to update the neural networks, focusing the training on problematic regions of the state space. This process continues until all conditions are provably satisfied. In the following subsections, we present our approach for learning storage and supply rate functions, and the complete verification procedure.

4.1 Learner of Storage and Supply Rate Functions

Dissipativity condition: Similarly to existing work on learning neural Lyapunov functions, $V(x)$, $Q(x)$, $S(x)$, and $R(x)$ are parameterized by feed-forward neural networks. However, unlike Lyapunov function training, which relies on *state samples* to satisfy stability conditions (2), the dissipativity condition (4b) requires training over *state-input samples*. This poses sampling challenges for systems with high control dimension m (e.g., fully or overly actuated systems). To mitigate this, we introduce a novel reformulation of (4b) that reduces the sampling space dimension.

Proposition 8 Consider the system (1), a storage

function $V(x)$ and a supply rate function $w(x, u) = x^\top Q(x)x + 2x^\top S(x)u + u^\top R(x)u$. If for all $x \in \mathcal{X}$, it holds that

$$\underbrace{\begin{bmatrix} R(x) & S(x)^\top x - 0.5g(x)^\top \frac{\partial V(x)}{\partial x}^\top \\ \star & -\frac{\partial V(x)}{\partial x} f(x) + x^\top Q(x)x \end{bmatrix}}_{:=M(x)} \succ 0. \quad (22)$$

Then, (4b) holds.

PROOF. By multiplying $[u^\top \ 1]$ and $[u^\top \ 1]^\top$ on the left hand side and right hand side of the matrix $M(x)$ in (22), we obtain the dissipativity condition (4b).

Although (22) is a matrix positive definite condition, it only depends on x , therefore the dimension of sampling space has been reduced. We also note that the practical meaning of this transformation goes beyond computational efficiency. Consider the original dissipativity condition (4b); the sampling space for the states can be defined by the practitioners. However, one may lose the freedom of choosing the sampling space for the input. This is because the magnitude of the structured control $\pi(x)$ is not known *a priori*, but instead *a posteriori*. If the input sampling space is too small, $\pi(x)$ can lie out of this space, while if the sampling space is too large, redundant samples will be unavoidably added. Our formulation addresses this directly.

The loss functional $\mathcal{L}_d(\theta; \mathcal{D})$ for the condition (22) is defined as

$$\mathcal{L}_d(\theta; \mathcal{D}) := \frac{1}{N} \sum_{x_i \in \mathcal{D}} \text{ReLU}(\max \text{eig}(-M(x_i))), \quad (23)$$

where $\max \text{eig}(\cdot)$ is the operator for the maximal eigenvalue, θ is the parameter for the trainable neural networks, \mathcal{D} is the set of state samples and N is the number of samples. When $M(x_i) \succ 0, \forall x_i \in \mathcal{D}$, the maximal eigenvalue for each $-M(x_i)$ is negative, then $\mathcal{L}_d = 0$. Otherwise, we have $\mathcal{L}_d > 0$. Note that the logarithm determinant barrier function $-\log \det(\cdot)$ has been widely used in convex optimization literature for positive semi-definite constraints [33]. The $\max \text{eig}(\cdot)$ is also convex, and always well-defined for any real symmetric matrix.

Storage function properties: We then consider the condition (4a), which requires the storage function $V(x)$ to be locally positive definite. $V(x)$ is parameterized by

$$V(x) = x^\top \tilde{V}(x), \quad (24)$$

where $\tilde{V}(x) : \mathcal{X} \rightarrow \mathbb{R}^{n \times n}$ is parameterized by a feed-forward neural network. Under this parameterization,

we immediately have that $V(0) = 0$ holds. Instead of enforcing $V(x)$ to be positive-definite, we consider a stronger condition which requires $V(x)$ to be bi-Lipshitz:

$$\mu x^\top x \leq V(x) \leq \nu x^\top x$$

where $0 < \nu < \mu$ are constants. The role of the lower bound $\mu x^\top x$ guarantees $V(x)$ is *strictly positive* for $x \neq 0$. Moreover, it eliminates local minima due to numerical precisions, in the sense that the value of $V(x)$ will not be too small for a state that is far away from the origin. On the contrary, the upper bound $\nu x^\top x$ guarantees that the value of $V(x)$ will not be too large for small x .

This loss functional \mathcal{L}_v for the condition (4a) is given by

$$\mathcal{L}_v(\theta; \mathcal{D}) := \frac{1}{N} \sum_{x_i \in \mathcal{D}} \{ \text{ReLU}(\mu x_i^\top x_i - V(x_i)) + \text{ReLU}(V(x_i) - \nu x_i^\top x_i) \}. \quad (25)$$

QSR-form supply rate properties: The next one is $\Delta(x) \succ 0$ in (7). Similarly to the treatment of the matrix inequality (22), we introduce the following loss functional

$$\mathcal{L}_t(\theta; \mathcal{D}) := \frac{1}{N} \sum_{x_i \in \mathcal{D}} \text{ReLU}(\max \text{eig}(-\Delta(x_i))). \quad (26)$$

The last constraint is $R(x) \succ 0$, which is integrated by the following loss functional

$$\mathcal{L}_r(\theta, \mathcal{D}) := \frac{1}{N} \sum_{x_i \in \mathcal{D}} \text{ReLU}(\max \text{eig}(-R(x_i))). \quad (27)$$

The overall loss function for learning the storage function and supply rate function is given by

$$\mathcal{L}(\theta, \mathcal{D}) := w_1 \mathcal{L}_d + w_2 \mathcal{L}_v + w_3 \mathcal{L}_t + w_4 \mathcal{L}_r, \quad (28)$$

where $w_1, \dots, w_4 > 0$ are weights.

Cost functional shaping One additional objective to be considered is cost functional shaping. In practice, one may want to optimize over a certain cost function $l(x, u)$ rather than the one derived in (18). Let $\bar{l}(x, u) := \tilde{l}(x, u) + u^\top R(x)u + x^\top \Delta(x)x$ denote the cost function of (18). Then, the cost function shaping can be achieved by considering a new loss function term with a set of sampled input-state \mathcal{D}' :

$$\mathcal{L}_c = \frac{1}{N} \sum_{x_i, u_i \in \mathcal{D}'} (l(x_i, u_i) - \bar{l}(x_i, u_i))^2. \quad (29)$$

This additional loss can be integrated into \mathcal{L} with a weight w_5 . When $l(x, u)$ is quadratic in u , the input sam-

Algorithm 1 Training Structured Neural Controllers

- 1: **Input:** training data set \mathcal{D} , region of interest \mathcal{X} , plant dynamics $f(x)$ and $g(x)$, PGD stepsize α and learning rate γ .
 - 2: **Output:** controller $\pi(x)$, storage function $V(x)$, QSR-form supply rate function $w(x, u)$
 - 3: **Initialize:** Neural networks $Q(x), S(x), R(x), \tilde{V}(x)$ parameterized with θ
 - 4: **repeat**
 - 5: **for** $iter = 1, 2, \dots$ **do**
 - 6: Randomly sample states $\tilde{x}_j \in \mathcal{X}$
 - 7: **for** $j = 1, 2, \dots$ **do**
 - 8: $\tilde{x}_j \leftarrow \text{Project}_{\mathcal{X}} \left(\tilde{x}_j + \alpha \cdot \frac{\partial \mathcal{L}(\theta; \tilde{x}_j)}{\partial \tilde{x}} \right)$
 - 9: **end for**
 - 10: $\mathcal{D} \leftarrow \{\tilde{x}_i\} \cup \mathcal{D}$
 - 11: **for** $epoch = 1, 2, \dots$ **do**
 - 12: $\theta \leftarrow \theta - \gamma \nabla_{\theta} \mathcal{L}(\theta, \mathcal{D})$
 - 13: **end for**
 - 14: **end for**
 - 15: **until** Passed the verifier
 - 16: $\pi(x) \leftarrow -R(x)^{-1}S(x)^\top x$
-

ples u_i is not needed for \mathcal{L}_c , as one can directly minimize the discrepancy for the coefficients of u in $l(x, u)$ and $\bar{l}(x, u)$.

4.2 Complete Verification and Counterexample Generation

We employ SMT (Satisfiability Modulo Theory) solvers to verify that our learned storage function $V(x)$ and QSR-form supply rate function $w(x, u)$ are valid and satisfy the dissipativity conditions. Using SMT solvers is a powerful technique for checking whether mathematical formulas hold over the domain of interest. For each candidate storage function $V(x)$ and supply rate $w(x, u)$, we verify three key conditions: 1) the bi-Lipschitz condition for $V(x)$; 2) the dissipativity condition $\dot{V}(x, u) \leq w(x, u)$; 3) the supply rate condition $R(x) \succ 0, \Delta(x) \succ 0$.

The existing SMT solvers such as dReal [17] do not directly support semi-definite constraints in the form of (22). To overcome this problem, we reformulate the matrix inequality constraints (22), (7) and $R(x) \succ 0, \forall x \in \mathcal{X}$ into equivalent and verifiable algebraic constraints.

For (22), consider the Schur complement for the first block $R(x)$, we have an equivalent but verifiable condition

$$\begin{aligned} & -\frac{\partial V(x)}{\partial x} f(x) + x^\top Q(x)x - S(x)^\top x \\ & + 0.5g(x)^\top \frac{\partial V(x)}{\partial x}^\top R(x)^{-1} \star > 0, \forall x \in \mathcal{X} \end{aligned} \quad (30)$$

The constraint (7) can be transformed into

$$x^\top \Delta(x)x > 0, \forall x \in \mathcal{X}. \quad (31)$$

The constraint $R(x) \succ 0, \forall x \in \mathcal{X}$ can be transformed into

$$x^\top R(x)x > 0, \forall x \in \mathcal{X}. \quad (32)$$

When $R(x)$ is taken as a constant matrix instead of a functional one, the positive definiteness can directly be checked by computing the eigenvalues.

For other verifiers such as mixed-integer programming [19] and $\alpha\beta$ -crown [18], the loss function \mathcal{L} in (28) can directly be used for verification.

While SMT solvers can provide formal guarantees and counterexamples, the verification process can be computationally intensive due to complex symbolic calculations. Some verifiers like $\alpha\beta$ -crown offer efficient verification but may not support counterexample generation. Therefore, similar to existing works [14, 15], we employ a hybrid approach: before invoking computationally expensive SMT verification, we first use projected gradient descent (PGD) [34] to efficiently search for potential counterexamples by maximizing the violation of our conditions. For a given point \tilde{x}_j , we compute the gradient of our conditions $\mathcal{L}(\theta; \tilde{x}_j)$ with respect to \tilde{x}_j and take steps in the direction that potentially increases violation, while projecting back onto our domain of interest after each step.

The PGD-based search serves as a fast preliminary check before formal verification. When PGD finds points that likely violate our conditions, these points are added to the training set. This hybrid strategy significantly reduces the computational burden while maintaining the soundness of our approach: PGD helps quickly identify problematic regions for learning, while formal verification is used periodically to provide guarantees. The complete verification-guided learning process alternates between: 1) Using PGD to efficiently find potential violations; 2) Updating the neural networks based on these violations; 3) Periodically employing formal verification for the learned functions.

The training algorithm is shown in Algorithm 1. On Lines 6-10, counterexamples are generated using PGD and added to the training dataset \mathcal{D} . On Lines 11-13, the parameters of neural networks are updated. If the trained neural networks pass verification, the control law $\pi(x) = -R(x)^{-1}S(x)^\top x$ is guaranteed to stabilize the system.

5 Experiments

We evaluate the performance of our proposed framework across three benchmark environments: *Electric Circuit*, *Inverted Pendulum*, and *Rod on a Cart*.

Each experiment is designed to assess the framework’s stability guarantees and optimality in comparison with baseline approaches. The controller is trained using Algorithm 1, and the cost functional shaping is defined as in (29). Source code is available at <https://anonymous.4open.science/r/Learning-Dissipativity-Control-07B6>.

We compare our method against:

- Neural Control Lyapunov Function (NCLF) [11, 14, 15] : While these methods differ in their choice of verifiers and conditions for enlarging the region of attraction, they share the same fundamental approach of jointly learning both the controller and Lyapunov function to guarantee stability;
- NODE: Optimal control via Neural ODEs;
- OURS-NCFS: Our proposed dissipativity-based approach without the cost functional shaping term (29).

The controllers designed by OURS, NCLF, and OURS-NCFS are verified using dReal [17] under the same precision and region. All methods share identical training settings (e.g., optimizer, PGD step size, learning rate, and network sizes).

Method NODE designs the control by solving the optimal control problem

$$\begin{aligned} \pi(x) = \arg \min_{u(\cdot)} \int_0^\infty l(x, u) dt, \\ \text{subject to } \dot{x} = f(x) + g(x)u, \end{aligned}$$

where $l(x, u)$ is the user-defined objective function. Our method considers the shape of the loss function $\bar{l}(x, u)$ with respect to $l(x, u)$ via the loss function term (29). In the following experiments, the performance oriented cost function $l(x, u)$ is designed as

$$l(x, u) := x^\top x + u^\top u \quad (33)$$

The size of neural networks and region of interest for each task is shown in Table 1. By the number for neural networks $V(x)$, $Q(x)$, $S(x)$ we mean the number of neurons. All of these functions are parameterized by feed-forward neural networks with one hidden layer, using tanh as the activation function. For all the experiments, the matrix $R(x)$ are parameterized by one linear layer.

For method “OURS”, the loss function is defined by

$$\mathcal{L}(\theta, \mathcal{D}) = w_1 \mathcal{L}_d + w_2 \mathcal{L}_v + w_3 \mathcal{L}_t + w_4 \mathcal{L}_r + w_5 \mathcal{L}_c$$

where the loss functions are given by (25) - (29). The neural control is then trained using Algorithm 1. For method “OURS-NCFS”, the loss function is defined by

$$\mathcal{L}(\theta, \mathcal{D}) = w_1 \mathcal{L}_d + w_2 \mathcal{L}_v + w_3 \mathcal{L}_t + w_4 \mathcal{L}_r,$$

Plant	Controller	$V(x)$	$Q(x)$	$S(x)$	$R(x)$	Region of interest
Pendulum	Static	8	8	8	Linear	$[\pi, 2]$
Pendulum	Dynamic	32	32	32	Linear	$[\pi, 2, 1]$
RodCart	Static	20	20	20	Linear	$[0.1, 0.1, 0.1, 0.1]$
Circuit	Static	8	8	8	Linear	$[1, 1]$

Table 1

Size of neural networks, type of controller and the region of interest for each task.

and the neural control is trained using Algorithm 1 with the same hyperparameters as “OURS”. For method “NCLF”, the neural Lyapunov function is parameterized in the same way as the storage function for “OURS” and “OURS-NCFS”. The neural controls for methods “NCLF” and “NODE” are trained as neural networks that always have the same numbers of hidden layers and neurons as $S(x)$. This guarantees that the neural controls for all the methods have the same numbers of parameters.

dReal [17] is selected as the verifier in Algorithm 1. The numerical precision δ is set to be 10^{-3} for all the experiments. We want to highlight here our method *does not* depend on the specific verifier, allowing the users to implement their own verification methods for formal dissipativity and stability guarantees.

To demonstrate optimality, we consider the following user-defined objective function

$$\int_0^\infty (l(x, u) := x^\top x + u^\top u) dt \quad (34)$$

where $x = [\theta \ \dot{\theta}]$ is the state, and u is the control input. After training the four controls, we evaluate the objective function (34) along the four closed-loop systems:

$$\dot{x} = f(x) + g(x)\pi_{\{\cdot\}}(x), \quad (35)$$

where $\{\cdot\} \in \{\text{OURS}, \text{NCLF}, \text{OURS} - \text{NCFS}, \text{NODE}\}$. In practice, the ordinary differential equations (35) are digitalized and solved using fourth-order Runge-Kutta (rk4) method. For each system, the temporal state-input pairs are sampled as

$$\{x(0), \pi_{\{\cdot\}}(0)\}, \{x(1), \pi_{\{\cdot\}}(1)\}, \dots, \{x(T), \pi_{\{\cdot\}}(T)\}, \quad (36)$$

and the empirical value is evaluated by

$$\sum_{t=0}^T x(t)^\top x(t) + \pi_{\{\cdot\}}(t)^\top \pi_{\{\cdot\}}(t). \quad (37)$$

The sequence (36) is sampled to be long enough $T \gg 0$, such that $x(T) = 0, \pi_{\{\cdot\}}(T)$ is ensured.

5.1 Electrical Circuit

In the electrical circuit experiment, we evaluate the stability and dissipativity properties of the control designed by our method. Since this is a linear system, we compare our method to the Linear Quadratic Regulator (LQR) with cost function (33), the theoretical optimal control solution for such systems. By applying our cost shaping method, we find that our framework successfully replicates the LQR solution as shown in Figure 2(a) and Table 2, achieving not only stability but also optimality with respect to the specified performance metric. While NODE appears to achieve a lower cost when evaluated on specific trajectory lengths during training and testing, the learned controller *fails to stabilize the system*. This exposes a key limitation of trajectory-based training: it optimizes performance over predefined trajectories but lacks guarantees of stability for the entire state space. In contrast, our dissipativity-based framework explicitly enforces stability guarantees, ensuring that the system converges robustly, even beyond the training scenarios.

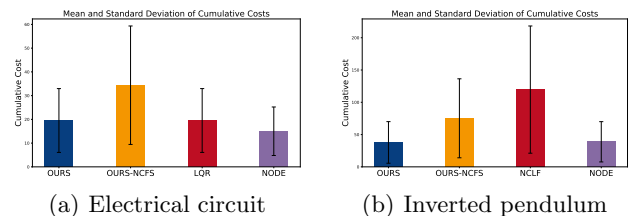


Fig. 2. The average empirical cumulative cost with standard deviation on 30 trials starting from random initial states.

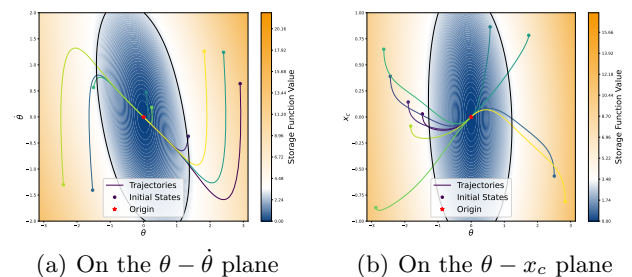


Fig. 3. The region of attraction (black contour) and the trajectories (colourful lines) of the closed-loop system.

Table 2

Empirical cumulative costs across different environments, averaged over 30 trials per method

	Cost				Stability Guarantee
	Circuit	Pendulum-static	Pendulum-dynamic	Rod on the Cart	
NCLF	19.5 (LQR)	119.7	125.7	3191.2	✓
Ours-NCFS	34.4	75.2	42.5	412.9	✓
Ours	19.5	37.8	15.1	361.3	✓
NODE	15.0	38.8	13.7	284.0	✗

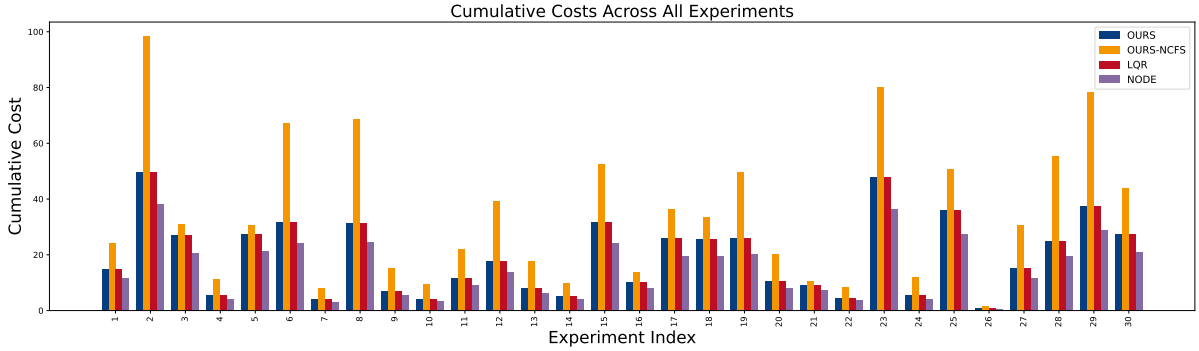


Fig. 4. Comparison of empirical cumulative costs (37) for the Electrical Circuit with static control.

5.2 Inverted Pendulum

The inverted pendulum system has state $x = [\theta, \dot{\theta}]$ where θ is the angle and $\dot{\theta}$ is the angular velocity. The control objective is to stabilize the pendulum around the upright position.

As shown in Figure 2(b) and Table 2, our approach not only ensures stability but also achieves better optimality than the other methods, even NODE which solves the optimal control problem.

We further extend our framework beyond static state feedback control to include dynamic control, which incorporates mechanisms like proportional-integral controllers. Dynamic controllers differ from static state feedback in that they consider not only the current state of the system but also past states or control actions, providing additional flexibility and improved performance for systems with memory or delayed responses. This formulation is detailed in Appendix A, where we show that the approach studied in [27] can be viewed as a special case of our framework. As shown in Figure 3, the learned storage function and supply rate demonstrate that our method stabilizes the closed-loop system. This highlights the ability of our approach to enforce theoretical guarantees effectively.

We evaluate our method alongside baselines under the dynamic control setting. As shown in Table 2, our method - both with and without cost function shap-

ing - outperforms NCLF. This advantage likely comes from the fact that NCLF lacks guarantees of optimality, which can lead to augmented control signals and augmented states becoming large in dynamic controllers. For the static and dynamic feedback cases, our method achieves optimality comparable to or even better than NODE. However, NODE still suffers from the absence of stability guarantees.

5.3 Rod on the Cart

We consider a flexible rod mounted on a moving cart, consisting of a cart with a metal rod fixed on top and a mass at the rod’s end. Unlike traditional cart-pole systems, the rod has no joint at its base but is flexible, allowing horizontal displacement between its top and bottom positions. This case is taken from [28].

The controller designed by our framework ensures fast convergence and smooth control behaviour, effectively stabilizing the flexible rod in the upright position. In terms of optimality, our method significantly outperforms NCLF, as shown in Table 2. This is likely due to the fact that NCLF lacks transient performance optimization, which can lead to overshooting in the designed controller. In contrast, our dissipativity-based approach inherently incorporates optimality, particularly when cost function shaping is applied, ensuring both stability and efficient control performance.

Table 2 and Figure 4 present a comprehensive cost comparison across all methods for the three systems. For

each system, we conduct 30 trials with random initial conditions within the specified region of interest. The consistent low costs achieved by OURS validate the optimality of our control design.

It is worth noting that even without cost function shaping, our method inherently guarantees closed-loop stability and a certain level of optimality due to its dissipativity-based design. This is reflected by the results, where our method always outperforms NCLF in optimality. The addition of cost function shaping further enhances our framework by allowing it to adapt to a specified cost function, effectively solving particular optimal control problems.

These results emphasize the key advantage of our dissipativity-based approach: dissipativity not only ensures closed-loop stability through energy-consistent behaviour but also provides guarantees of optimality, with or without cost shaping. The cost shaping extension broadens the applicability of the framework to handle customized performance objectives, bridging stability and performance in a unified framework.

6 Conclusion

We proposed a novel framework for designing optimal stabilizing control for nonlinear systems by learning the system’s input-output dissipativity. Unlike existing learning-based control methods, our approach ensures both stability and superior optimality by design, as demonstrated on linear and nonlinear system examples.

While our reformulation reduces the sampling space dimension, learning storage and supply rate functions remains challenging due to multiple hard constraints that must be handled during training. These constraints are enforced via appropriate loss functions. Recent work on direct parameterization of robust neural networks [35] suggests a promising direction. We plan to explore parameterizing storage and supply rate functions with neural networks to enforce some constraints by design.

Acknowledgement

The authors thank Professors Kostas Margellos, Alessandro Abate and Konstantinos Gatsis for fruitful discussions.

References

[1] C. Tang, B. Abbatematteo, J. Hu, R. Chandra, R. Martín-Martín, and P. Stone, “Deep reinforcement learning for robotics: A survey of real-world successes,” *Annual Review of Control, Robotics, and Autonomous Systems*, vol. 8, 2024.

[2] A. Haydari and Y. Yılmaz, “Deep reinforcement learning for intelligent transportation systems: A survey,” *IEEE Transactions on Intelligent Transportation Systems*, vol. 23, no. 1, pp. 11–32, 2020.

[3] Y. Zhang, X. Shi, H. Zhang, Y. Cao, and V. Terzija, “Review on deep learning applications in frequency analysis and control of modern power system,” *International Journal of Electrical Power & Energy Systems*, vol. 136, p. 107744, 2022.

[4] S. Sastry, *Nonlinear systems: analysis, stability, and control*, vol. 10. Springer Science & Business Media, 2013.

[5] L. Yang, H. Dai, A. Amice, and R. Tedrake, “Approximate optimal controller synthesis for cart-poles and quadrotors via sums-of-squares,” *IEEE Robotics and Automation Letters*, 2023.

[6] H. Dai and F. Permenter, “Convex synthesis and verification of control-lyapunov and barrier functions with input constraints,” in *2023 American Control Conference (ACC)*, pp. 4116–4123, IEEE, 2023.

[7] J. Anderson and A. Papachristodoulou, “Advances in computational lyapunov analysis using sum-of-squares programming,” *Discrete & Continuous Dynamical Systems-Series B*, vol. 20, no. 8, 2015.

[8] A. Papachristodoulou and S. Prajna, “On the construction of lyapunov functions using the sum of squares decomposition,” in *Proceedings of the 41st IEEE Conference on Decision and Control, 2002.*, vol. 3, pp. 3482–3487, IEEE, 2002.

[9] A. A. Ahmadi and B. El Khadir, “A globally asymptotically stable polynomial vector field with rational coefficients and no local polynomial lyapunov function,” *Systems & Control Letters*, vol. 121, pp. 50–53, 2018.

[10] R. Zhou, T. Quartz, H. De Sterck, and J. Liu, “Neural lyapunov control of unknown nonlinear systems with stability guarantees,” *Advances in Neural Information Processing Systems*, vol. 35, pp. 29113–29125, 2022.

[11] Y.-C. Chang, N. Roohi, and S. Gao, “Neural lyapunov control,” *Advances in neural information processing systems*, vol. 32, 2019.

[12] S. Chen, M. Fazlyab, M. Morari, G. J. Pappas, and V. M. Preciado, “Learning lyapunov functions for piecewise affine systems with neural network controllers,” *arXiv preprint arXiv:2008.06546*, 2020.

[13] H. Dai, B. Landry, L. Yang, M. Pavone, and R. Tedrake, “Lyapunov-stable neural-network control,” *arXiv preprint arXiv:2109.14152*, 2021.

[14] L. Yang, H. Dai, Z. Shi, C.-J. Hsieh, R. Tedrake, and H. Zhang, “Lyapunov-stable neural control for state and output feedback: A novel formulation,” in *Forty-first International Conference on Machine Learning*, 2024.

[15] J. Wu, A. Clark, Y. Kantaros, and Y. Vorobeychik, “Neural lyapunov control for discrete-time systems,” *Advances in neural information processing systems*, vol. 36, pp. 2939–2955, 2023.

[16] A. Abate, C. David, P. Kesseli, D. Kroening, and E. Polgreen, “Counterexample guided inductive synthesis modulo theories,” in *International Conference on Computer Aided Verification*, pp. 270–288, Springer, 2018.

[17] S. Gao, S. Kong, and E. M. Clarke, “dreal: An smt solver for nonlinear theories over the reals,” in *International conference on automated deduction*, pp. 208–214, Springer, 2013.

[18] S. Wang, H. Zhang, K. Xu, X. Lin, S. Jana, C.-J. Hsieh, and J. Z. Kolter, “Beta-crown: Efficient bound propagation with per-neuron split constraints for neural network robustness verification,” *Advances in Neural Information Processing Systems*, vol. 34, pp. 29909–29921, 2021.

- [19] V. Tjeng, K. Xiao, and R. Tedrake, "Evaluating robustness of neural networks with mixed integer programming," *arXiv preprint arXiv:1711.07356*, 2017.
- [20] M. Fazlyab, M. Morari, and G. J. Pappas, "Safety verification and robustness analysis of neural networks via quadratic constraints and semidefinite programming," *IEEE Transactions on Automatic Control*, vol. 67, no. 1, pp. 1–15, 2020.
- [21] J. C. Willems, "Dissipative dynamical systems part i: General theory," *Archive for rational mechanics and analysis*, vol. 45, no. 5, pp. 321–351, 1972.
- [22] P. Moylan and B. Anderson, "Nonlinear regulator theory and an inverse optimal control problem," *IEEE Transactions on Automatic Control*, vol. 18, no. 5, pp. 460–465, 1973.
- [23] L. Grüne, "Dissipativity and optimal control: Examining the turnpike phenomenon," *IEEE Control Systems Magazine*, vol. 42, no. 2, pp. 74–87, 2022.
- [24] M. Lanchares and W. M. Haddad, "Nonlinear optimal control for stochastic dynamical systems," *Mathematics*, vol. 12, no. 5, p. 647, 2024.
- [25] D. d. S. Madeira, "Necessary and sufficient dissipativity-based conditions for feedback stabilization," *IEEE Transactions on Automatic Control*, vol. 67, no. 4, pp. 2100–2107, 2022.
- [26] K. S. Schweidel and M. Arcak, "Compositional analysis of interconnected systems using delta dissipativity," *IEEE Control Systems Letters*, vol. 6, pp. 662–667, 2021.
- [27] W. Cui, Y. Jiang, B. Zhang, and Y. Shi, "Structured neural-pi control with end-to-end stability and output tracking guarantees," *Advances in Neural Information Processing Systems*, vol. 36, 2024.
- [28] N. Junnarkar, M. Arcak, and P. Seiler, "Synthesizing neural network controllers with closed-loop dissipativity guarantees," *arXiv preprint arXiv:2404.07373*, 2024.
- [29] Y. Xu and S. Sivaranjani, "Learning dissipative neural dynamical systems," *IEEE Control Systems Letters*, vol. 7, pp. 3531–3536, 2023.
- [30] Z. Li, M. Liu-Schiaffini, N. Kovachki, K. Azizzadenesheli, B. Liu, K. Bhattacharya, A. Stuart, and A. Anandkumar, "Learning chaotic dynamics in dissipative systems," *Advances in Neural Information Processing Systems*, vol. 35, pp. 16768–16781, 2022.
- [31] Y. Okamoto and R. Kojima, "Learning deep dissipative dynamics," *arXiv preprint arXiv:2408.11479*, 2024.
- [32] R. Sepulchre, M. Jankovic, and P. V. Kokotovic, *Constructive nonlinear control*. Springer Science & Business Media, 2012.
- [33] S. Boyd, "Convex optimization," *Cambridge UP*, 2004.
- [34] A. Madry, "Towards deep learning models resistant to adversarial attacks," *arXiv preprint arXiv:1706.06083*, 2017.
- [35] R. Wang and I. Manchester, "Direct parameterization of lipschitz-bounded deep networks," in *International Conference on Machine Learning*, pp. 36093–36110, PMLR, 2023.
- [36] A. Visioli, *Practical PID control*. Springer Science & Business Media, 2006.
- [37] J. W. Simpson-Porco, "Equilibrium-independent dissipativity with quadratic supply rates," *IEEE Transactions on Automatic Control*, vol. 64, no. 4, pp. 1440–1455, 2018.
- [38] D. d. S. Madeira and T. A. Lima, "Global stabilization of polynomial systems using equilibrium-independent dissipativity," in *2022 American Control Conference (ACC)*, pp. 120–125, IEEE, 2022.

A Dynamic Control Design

Dynamic control is widely used in control theory. One example is proportional-integral-derivative (PID) control, which is well-known for its capability of fast convergence (proportional), eliminating tracking errors (integral) and reducing overshoot (derivative). For linear systems, these three parts are designed linearly over states, error and the integral of states [36]. The paradigm has been extended to nonlinear PI control for nonlinear systems, and the control can be designed with learning techniques [27]. Here, we propose a universal framework for dynamic controller design to enable more flexible and efficient operation. The diagram of the plant and the controller is shown as follows.

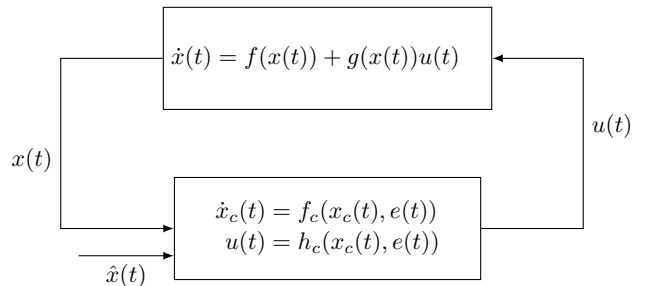


Fig. A.1. Overall system framework: interconnected dynamical system and control system. The block on the top represents the plant, and the one on the bottom represents the controller. In the controller dynamics, $e(t) := \hat{x}(t) - x(t)$ represents the tracking error, where $\hat{x}(t)$ is a reference signal.

Compared with the static control design Framework 1, the dynamic control design Framework A.1 introduces auxiliary state x_c for the controller dynamics. The closed-loop system can be regarded as an interconnected system with a dynamical plant and a dynamical controller. The interconnected system can be represented by the state-space model:

$$\underbrace{\begin{bmatrix} \dot{x} \\ \dot{x}_c \end{bmatrix}}_{x_e} = \underbrace{\begin{bmatrix} f(x) \\ 0 \end{bmatrix}}_{f_e(x_e)} + \underbrace{\begin{bmatrix} 0 & g(x) \\ I & 0 \end{bmatrix}}_{g_e(x_e)} \underbrace{\begin{bmatrix} f_c(x_c, e) \\ h_c(x_c, e) \end{bmatrix}}_{u_e(x_e, e)}, \quad y_e = h_e(x_c, e). \quad (\text{A.1})$$

Here, $h_e(x_c, e)$ is a *user-defined* virtual output function, which satisfies $h_e(0, 0) = 0$. The control takes the form of $u_e = \pi(x_c, e)$ that stabilizes the plant. We first consider the equilibrium point $\bar{x}_e = [\bar{x} \quad \bar{x}_c]$ and $\bar{u}_e = [\bar{u}_c \quad \bar{u}]$. At the equilibrium point \bar{x}_e , we should have $\dot{\bar{x}}_e = 0$, which implies

$$\begin{aligned} f(\bar{x}) + g(\bar{x})\bar{u} &= 0 \\ \bar{u}_c &= 0 \end{aligned} \quad (\text{A.2})$$

The dissipativity condition (4b) can be extended for the augmented system (A.1) with a non-zero equilibrium

point \bar{x}_e :

$$\begin{aligned} \nabla V_e(\bar{x}_e)^\top [f_e(x_e) + g_e(x_e)u_e] + &\leq (\bar{y}_e - y_e)^\top Q(\bar{x}_e)(\bar{y}_e - y_e) \\ + 2(\bar{y}_e - y_e)^\top S(\bar{x}_e)(\bar{u}_e - u_e) + &(\bar{u}_e - u_e)^\top R(\bar{x}_e)(\bar{u}_e - u_e). \end{aligned} \quad (\text{A.3})$$

A similar condition has been presented in [37, 38] for static feedback control.

Similarly to the static control (8), the nonlinear dynamical control u_e is given by

$$u_e = \bar{u}_e - R(\bar{x}_e)^{-1}S(\bar{x}_e)^\top y_e, \quad (\text{A.4})$$

where \bar{u}_e is a feedforward compensator, $-R^{-1}S(\bar{x}_e)y_e$ is the nonlinear dynamical controller. For the special case where $y_e = x_e$, the nonlinear dynamical controller u_e becomes a state feedback control

$$u_e = \bar{u}_e - R(\bar{x}_e)^{-1}S(\bar{x}_e)^\top x_e.$$

If (A.3) and additionally $\Delta(\bar{x}_e) = S(\bar{x}_e)R(\bar{x}_e)^{-1}S(\bar{x}_e)^\top - Q(\bar{x}_e) \succ 0$ hold for any x and x_c , then stability of the augmented system (A.1) with u_e in (A.4) is guaranteed using Theorem 5.

Moreover, the proposed dynamical control is a generalization of nonlinear PI control. To see this, by letting

$$\begin{aligned} f_c(x_c(t), e(t)) &= e(t), \\ h_c(x_c(t), e(t)) &= k_I(x_c(t)) + k_p(e(t)) \end{aligned} \quad (\text{A.5})$$

the controller dynamics become

$$\begin{aligned} x_c(t) &= \int_0^t e(\tau) d\tau \\ u(t) &= k_I(x_c(t)) + k_p(e(t)), \end{aligned} \quad (\text{A.6})$$

where x_c has a clear physical meaning, *cumulative tracking error*, $k_I(x_c(t))$ is then the nonlinear integral control and $k_p(e(t))$ is the nonlinear proportional control. Neural nonlinear PI control in the form of (A.6) has been considered in [27]. Framework A.1 extends it.